Transverse Modal Vibrations
of Vertical Tensioned Risers

A Simplified Analytical Approach*

C.P. Sparks[1]

1 Institut français du pétrole, division Mécanique appliquée, 1 et 4, avenue de Bois-Préau, 92852 Rueil-Malmaison Cedex - France
e-mail: charles.sparks@ifp.fr

Résumé — **Vibrations transverses modales de risers verticaux tendus. Approche analytique simplifiée** — Le présent article est consacré à l'analyse structurelle des vibrations transverses modales d'un riser vertical tendu. Ces vibrations, souvent de type VIV (*Vortex Induced Vibrations*), apparaissent en présence d'un courant lorsque la fréquence des lâchers tourbillonnaires coïncide avec une des fréquences propres de la structure.

Une approche analytique simplifiée est proposée pour le cas d'un riser possédant des caractéristiques de poids apparent et de masse linéique uniformes. Des formules très simples sont ainsi obtenues pour les paramètres structurels les plus significatifs : fréquences propres, positions des nœuds et des ventres, débattements angulaires en tête et en pied, valeurs et positions des points de courbure maximale.

Les formules obtenues permettent de mieux comprendre la réponse structurelle d'un riser en eau profonde en condition dite « d'accrochage », pour le phénomène de VIV.

Mots-clés : riser, vibration, VIV.

Abstract — ***Transverse Modal Vibrations of Vertical Tensioned Risers. A simplified Analytical Approach*** — *The paper examines the physics of riser transverse modal vibrations of the type induced by VIV (Vortex Induced Vibrations). It presents a simplified analytical solution for such vibrations of vertical tensioned risers with uniform linear characteristics. The solution leads to simple expressions for the principal factors of concern including the natural frequencies, the positions of the nodes and anti-nodes, the maximum angular movements at the riser lower end, and the positions and values of maximum riser curvature.*

The expressions increase understanding of VIV of deepwater risers under "lock-in" conditions.

Keywords: riser, vibration, VIV.

NOMENCLATURE

E	Young's modulus
I	sectional inertia
L	riser length
L_n	length between nodes
S_t	Strouhal number
T_a	effective tension at anti-node
T_b	effective tension at riser bottom end
T_t	effective tension at riser top end
T_x	effective tension at height x
T_{pn}	nth mode natural period
U	current velocity
Y_x	modal shape
Y_a	modal amplitude
a	anti-node number
c	celerity of riser transverse waves
c_{Rm}	riser mean celerity
c_m	mean celerity between nodes
f_s	Strouhal frequency (Hz)
g	gravitational acceleration
k	intermediate node number
m	linear mass (including added mass)
n	mode number
t	time
w	apparent linear weight
x	distance - vertical axis
y	distance - horizontal axis
z	a dimensionless parameter
ϕ	phase angle (radians)
θ_b	riser bottom end angle
ω_n	nth Mode circular frequency (rad/s).

INTRODUCTION

Vortex induced vibration (VIV) of risers is a subject of increasing concern as drilling and production operations move into ever deeper waters. Riser designers and operators are aware that VIV may cause unacceptable levels of fatigue damage to deepwater risers. A large body of literature on the subject is now available. To cite only a part: an overview of the subject is presented in [1]. Experimental data acquired on real deepwater risers as part of the "Norwegian Deepwater Programme" and on the Schiehallion riser have been published in [2-5].

Methods of optimising natural damping, by deliberately staggering riser joints of different diameters, have been explored in [6] and [7]. The possibility of coupling between transverse and axial responses at very high modes has been reported in [8].

The experimental data on very deep risers mentioned above are particularly significant and have so far shown the response of the four instrumented risers [2-5] to be principally at low Modes (1 to 4). Greatest responses reported are single-mode, where amplitudes of the order of 0.5-1 diameters are mentioned. Multi-mode responses have also been observed but with lesser amplitudes. VIV "lock-in" was recorded in the 2nd Mode of the "Helland-Hansen" riser, with a modal period of about 20 s.

A clear understanding of deepwater riser modal response is important. It is the ambition of this paper to contribute to that understanding. The approach used is "simplified analysis" applied to a vertical riser with uniform characteristics of linear mass (including added mass), linear apparent weight and hydraulic diameter. The riser is assumed to be connected to the sea floor and is free to rotate at its extremities.

Simple expressions are derived for all the parameters of major concern including:
– the natural frequencies and periods of the modes;
– the positions of the nodes and anti-nodes according to the mode excited;
– the angular movement at the riser foot;
– the curvature at the anti-nodes and particularly the lowest anti-node;
– the position and value of maximum curvature.

The expressions increase understanding of VIV response of deepwater vertical tensioned risers. It must be stressed however that they say nothing about the natural vibrations of other types of riser such as catenary risers, compliant vertical risers, closely spaced groups of vertical risers or hung-off risers.

Two approximations are involved in the "simplified analysis" presented in Section 4 of this paper. The first consists of neglecting the riser flexural rigidity (*EI*) and thus treating the riser as a tensioned "cable". This leads to a modal equation in terms of Bessel functions. The second approximation consists of making a slight modification to the "cable vibration equation" (already proposed in [9]) which leads to simpler expressions than those involving Bessel functions.

A way of modifying the solution of Section 4 to take into account flexural rigidity (*EI*) is explored in Section 5. The validity of the approximations is tested by comparing the results of the "simplified analysis" (with and without *EI*) with those of the "Bessel analysis", and also with results of the "Deeplines" commercial riser analysis program [10]—a finite element program based on a 3D version of Equation (2) of this paper. Comparisons are made in the Appendix for a severe case of a large diameter drilling riser, filled with heavy mud, operating with very low top tension.

Throughout this article all references to "tension" imply "effective tension".

1 BACKGROUND

Before proceeding further, basic points about transverse vibrations of vertical connected risers must be mentioned.

1.1 Undamped Transverse Vibrations

When an undamped riser is forced to vibrate transversely (for example by an imposed top end sinusoidal movement) transverse waves descend the riser, are reflected back at the riser foot, and then re-ascend the riser to the top end where they arrive out of phase (say by angle φ) with the exciting movement. At the top end they are reflected again and begin a second descent/re-ascent of the riser following which they arrive back at the top end, this time out of phase by 2φ with the exciting movement.

In the absence of damping these reflections continue indefinitely. Under sustained excitation a multitude of waves propagate along the riser, each out of phase with the previous one by an angle φ. The resultant fluctuates, but never exceeds the maximum effect of a train of π/φ waves. The cumulative effect of the remainder is zero since the waves cancel out.

The exception to the above is provided by *modal vibrations* for which the reflected waves are all in phase with each other (φ = 0). All descending waves are perfectly superimposed and cannot be distinguished from each other. Likewise for the ascending waves. Hence modal vibrations

are the resultant of the interaction between only two waves – one descending and one ascending.

Figure 1 illustrates the case of a riser with positive weight in water and very low top tension, vibrating in the third Mode. The figure shows the profiles of the riser (black) and of the descending and ascending waves (blue and red respectively) at eight equal time intervals *during a half modal period*. For clarity one wave crest of each of the two component waves is highlighted with beads. Figures 1a and 1i show the riser in the positions of "zero amplitude" where the descending and ascending waves are perfect mirror images of each other. They cancel completely and the riser is straight. In this position the "crests" of the ascending and descending waves pass each other at the nodes.

As the descending and ascending waves progress along the riser they evolve both in amplitude and wavelength (similarly to ocean waves approaching a shore). This is the result of the non-constant tension.

Figure 1e shows the riser in a position of "maximum amplitude" where the two waves combine perfectly and cannot be distinguished from each other. In this position the "crests" of the waves pass each other at the anti-nodes.

Fundamental to the rest of the paper is the fact that the time required for the descending and ascending waves to travel between adjacent nodes *(Fig. 1a to 1i)* is equal to *half the modal period*. Likewise the time for them to travel between a node and an adjacent anti-node (or vice versa) is
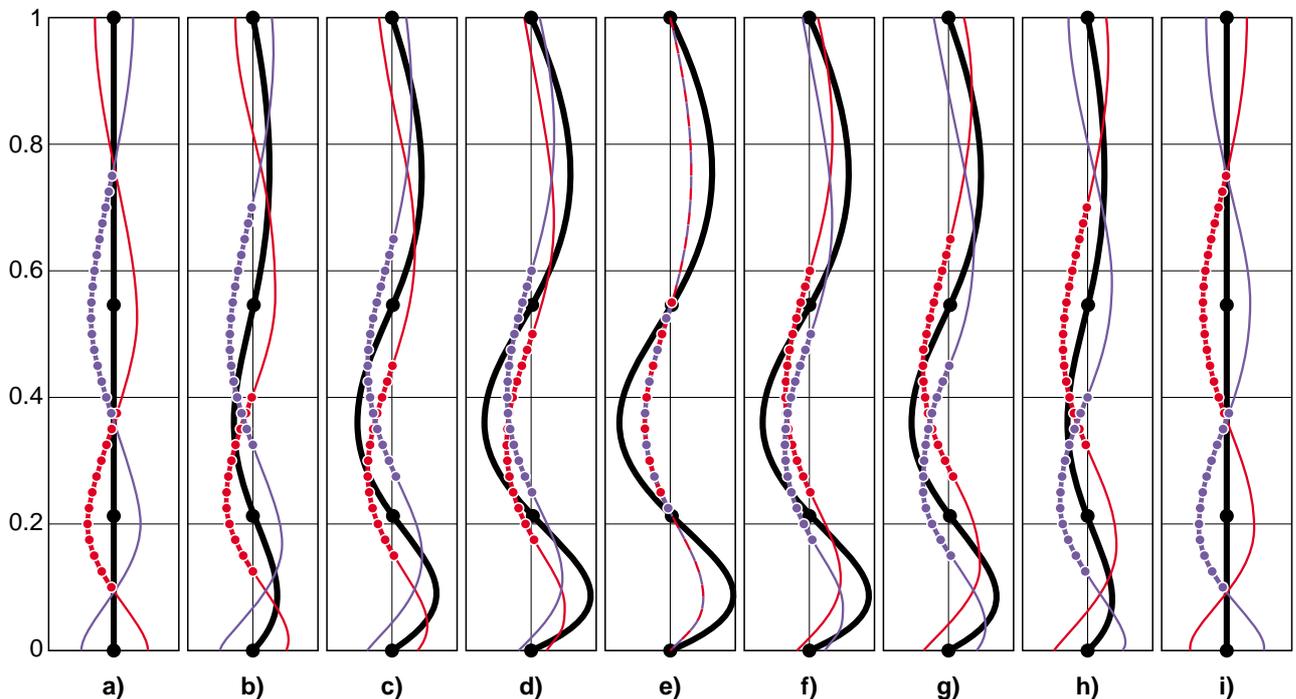

Figure 1

Third mode vibration of a riser with low top tension.

Evolution of descending wave (blue) and ascending wave (red) and the reulting riser profile during one half modal period.

equal to a *quarter of the modal period (Fig 1a to 1e and Fig. 1e to 1i)*. It follows that the period of the fundamental (Mode 1) is equal to the time required for the waves to travel twice the length of the riser.

1.2 VIV "Modal Vibrations"

Well documented experimental data relevant to VIV vibrations of risers *(see [11, 12])* have confirmed that the vortex shedding frequency for a fixed cylinder is a function of the ratio of current velocity to diameter as given by the Strouhal relation [13]:

$$f_s = S_t \frac{U}{D} \tag{1}$$

where the Strouhal number is generally about 0.2. However if the cylinder is elastically supported and has a natural frequency close to the one given by Equation (1) then the vortex shedding frequency will adapt itself to the natural frequency of the cylinder and the Strouhal relation will be modified. This situation is known as "lock-in".

Experimental data has shown that under "lock-in" conditions the cylinder vibrates at one of its natural frequencies, but with amplitudes auto-limited to about +/–1 diameter. For greater amplitudes the vortices cease to excite the motion. They have a damping effect. This limit in amplitude is also considered to apply to risers although real field data is sparse and difficult to interpret.

Hence when subjected to VIV, riser response at a natural frequency does not increase indefinitely, and amplitudes of the "peaks" of the lateral movement are all approximately equal. They do not increase with depth as given by the mode shape shown in Figure 1.

VIV "lock-in" on a riser causes the mode shape to be modified by a continual transfer of energy. This is continually added to the riser in the upper regions (where the modal amplitude would otherwise be smaller than the mean) and damped out from the lower regions (where the amplitudes would otherwise be greater than the mean).

2 BASIC EQUATIONS VIBRATION OF A TENSIONED BEAM

A riser is basically a vertical tensioned beam for which the equation of transverse vibration is as follows (see Figure 2 for riser axes):

$$EI \frac{d^4 y}{dx^4} - T_x \frac{d^2 y}{dx^2} - w \frac{dy}{dx} + m \frac{d^2 y}{dt^2} = 0 \tag{2}$$

Equation (2) only has an exact analytical solution for the case of *constant tension* ($w = 0$). The solution is then [14]:

$$y = Y_a \sin(\frac{n \pi x}{L}) \sin(\omega_n t) \tag{3}$$

Figure 2
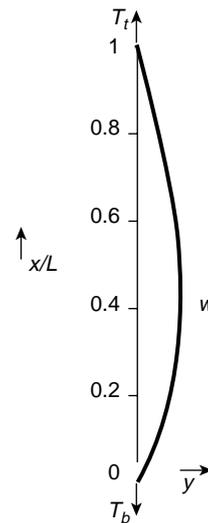
Riser axes.

The natural circular frequency ω_n and the natural period T_{P_n} for Mode "*n*" are then given by:

$$T_{p_n} = \frac{2\pi}{\omega_n} = \frac{2L / n}{\sqrt{\left\{ \frac{T}{m} + \left[(\frac{n\pi}{L})^2 \frac{EI}{m} \right] \right\}}} \tag{4}$$

Given that the transmission time of transverse waves between adjacent nodes is equal to half the modal period *(Section 1.1)*, Equation (4) can be rewritten as:

$$T_{p_n} = \frac{2L_n}{\sqrt{\left\{ c_{\text{cable}}^2 + c_{\text{beam}}^2 \right\}}} \tag{5}$$

where L_n is the length between nodes. And the "cable" and "beam" celerities are respectively:

$$c_{\text{cable}} = \sqrt{T / m} \tag{6}$$

$$c_{\text{beam}} = \left(\frac{\pi}{L_n} \right) \cdot \sqrt{\frac{EI}{m}} \tag{7}$$

Hence the celerity c' in the *tensioned beam* is given by:

$$c' = \sqrt{\left\{ c_{\text{cable}}^2 + c_{\text{beam}}^2 \right\}} \tag{8}$$

For a deepwater riser beam celerity is generally small compared to cable celerity and has little influence.

For example: for a steel riser of length 2000 m, diameter 22", thickness 1", linear mass 1.2 tonnes/m under 150 tonnes constant tension, vibrating in the 10th Mode: celerity is *c'* only 2.6% greater than c_{cable}.

For less severe cases such as risers of smaller diameter, with lower bending stiffness, vibrating at lower modes, with higher axial tensions, the influence of flexural rigidity is even less.

Hence flexural rigidity (*EI*) generally has small influence on the natural period of lateral vibrations of a vertical *weightless* deepwater riser except for very high modes. It is reasonable to expect the same to be true of vertical risers that are *not weightless* (with positive apparent weight in water). Hence as a first approximation the riser will be treated as a cable. This approximation has been justified in previous publications *(see [9])*.

3 MODAL VIBRATION
VERTICAL RISER WITHOUT FLEXURAL RIGIDITY
(*EI* = 0)

If flexural rigidity (*EI*) is neglected Equation (2) reduces to:

$$T_x \frac{d^2 y}{dx^2} + w \frac{dy}{dx} - m \frac{d^2 y}{dt^2} = 0 \tag{9}$$

Putting:

$$z_x = \left[\frac{2\sqrt{mT_x}}{w} \right] \omega_n \tag{10}$$

and putting

$$y = Y_x \sin(\omega_n t) \tag{11}$$

where Y_x is the mode shape, Equation (9) can be rewritten as:

$$\frac{d^2 Y_x}{dz^2} + \frac{1}{z} \frac{dY_x}{dz} + Y_x = 0 \tag{12}$$

This has solution:

$$Y_x = [A \cdot J_0(z_x) + B \cdot Y_0(z_x)] \tag{13}$$

where $J_0(z_x)$, $Y_0(z_x)$ are Bessel functions of the first and second kind of order zero. Constants *A* and *B* can be found by iteration since "*y*" is zero at the extremities.

Although Equations (11) and (13) give the exact solution of Equation (9) and hence an approximate solution of Equation (2), the solution is not of great practical value since Bessel functions are difficult to evaluate. They have been evaluated for the example in Appendix. For simplicity, in the rest of the paper, analysis based on Equation (13) is referred to as "Bessel analysis".

4 SIMPLIFIED ANALYSIS
VERTICAL RISER WITHOUT FLEXURAL RIGIDITY
(*EI* = 0)

A simpler expression *(than Eq. (13))* for the mode shape of a riser without flexural rigidity can be found by making a slight modification to Equation (9). This plainly needs to be done with great care if the results are to be of value. The validity of such a modification can be verified directly by comparing results with those obtained with the "Bessel analysis" *(Eq. (13))* and with results of the "Deeplines" riser analysis program. This is presented in Appendix for a particular example.

The three terms of Equation (9) represent lateral force components (per unit length) at a point "*x*" above the riser foot. Their physical significance must first be examined *(see Fig. 3)*.

The first term is the restoring force resulting from the effect of axial tension acting in the curved riser. This is opposed by the inertia force given by the last term. These forces are of constant direction between adjacent nodes.

The middle term is the result of the component of linear apparent weight perpendicular to the riser. Since the riser is near *vertical* this term must already be small. Furthermore this force component changes direction between nodes. Above the anti-node it acts with the first term *(see Fig. 3)*. Below the anti-node it opposes it. Its resultant when integrated between adjacent nodes is zero. Hence this term must be of much less significance than the other two.

Without further justification it is proposed to *halve* the middle term of Equation (9) in order to allow a simpler analytical solution:

$$T_x \frac{d^2 y}{dx^2} + \left(\frac{1}{2} \right) w \frac{dy}{dx} - m \frac{d^2 y}{dt^2} = 0 \tag{14}$$
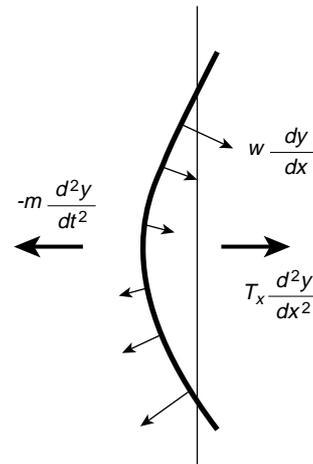

Figure 3

Force component acting between nodes.

using the substitutions given by Equations (10) and (11), Equation (14) becomes:

$$\frac{d^2 Y_x}{dz^2} + Y_x = 0 \qquad (15)$$

which has solution:

$$Y_x = Y_a \sin(z_x - z_b) \qquad (16)$$

where Y_a is the modal amplitude (a constant) and z_b is the value of z_x at the riser foot.

Figure 4

Riser 5th mode vibration. Comparison of mode shapes.

The amplitudes at the anti-nodes according to Equation (16) are all *equal* to Y_a. This is in contrast to the "Bessel expression" *(Eq. (13))* for which they increase in amplitude as they descend the riser *(see Fig. 4)*.

But since vertical tensioned risers subjected to VIV *do* tend to vibrate with virtually equal amplitudes at the anti-nodes, from the point of view of amplitude, the "simplified solution" *(Eq. (16))* is a closer representation of VIV induced modal response than the mathematically more exact "Bessel expression" of Equation (13).

Equation (16) allows a wealth of important parameters related to lateral vibrations of vertical tensioned risers to be calculated very easily.

4.1 Riser Natural Circular Frequencies and Natural Periods

The natural circular frequencies and periods can be found by considering the riser extremities where the lateral displacement "y" is zero. For Mode "n" Equation (16) gives:

$$z_t - z_b = n\pi \qquad (17)$$

where z_t and z_b are the values of "z" at the riser top and bottom ends. Noting that $wL = T_t - T_b$, substitution from Equation (10) yields:

$$\omega_n = \frac{n\pi}{2\sqrt{m}} \frac{w}{\left[\sqrt{T_t} - \sqrt{T_b}\right]} \qquad (18)$$

$$T_{p_n} = \frac{2\pi}{\omega_n} = \frac{4\sqrt{m}}{w} \left[\frac{\sqrt{T_t} - \sqrt{T_b}}{n}\right]$$
$$= \frac{4L / n}{\left[\sqrt{T_t / m} + \sqrt{T_b / m}\right]} \qquad (19)$$

Coherent units (such as SI units) must be used when evaluating ω_n or t_{p_n}.

4.2 Riser Mean Celerity

Since the period of the fundamental (first Mode) is equal to the time for transverse waves to travel twice the length of the riser *(Section 1.1)*, the riser mean celerity is:

$$c_{Rm} = \frac{2L}{T_{p_1}} \qquad (20)$$

Hence from Equation (19):

$$c_{Rm} = \frac{\sqrt{T_t / m} + \sqrt{T_b / m}}{2} \qquad (21)$$

Thus the riser mean celerity is the mean of the cable celerities at the upper and lower extremities.
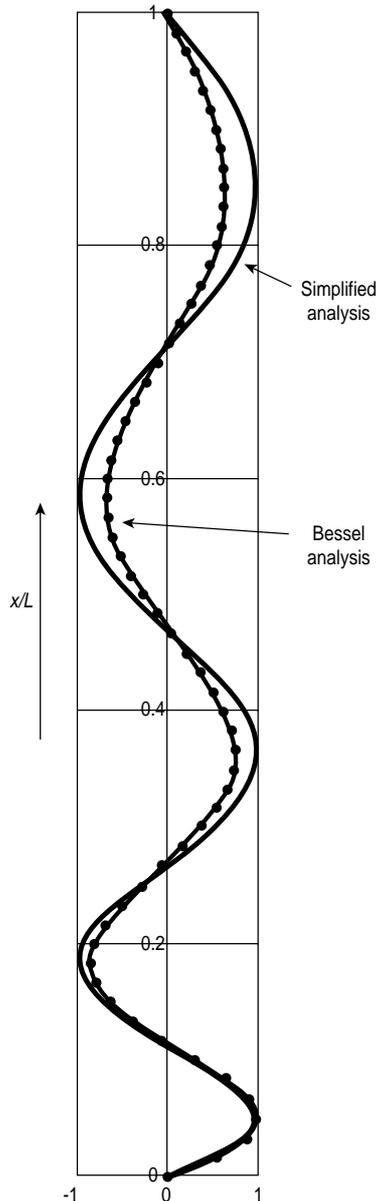
Finally the simplest way of determining the natural period of the fundamental (first Mode) is to calculate the mean celerity from Equation (21) and then determine the period of the fundamental (T_{p_1}) from:

$$T_{p_1} = \frac{2L}{c_{Rm}} \tag{22}$$

From Equation (19) the natural period for Mode "n" is then given by:

$$T_{p_n} = T_{p_1} / n \tag{23}$$

4.3 Evaluation of the Dimensionless Parameter z_x

The value of z_x at any point height x can be found from the corresponding tension (T_x) and the mode number. From Equation (10):

$$z_x = z_t \sqrt{T_x / T_t} = z_b \sqrt{T_x / T_b} \tag{24}$$

Thus from Equation (17):

$$z_x = \frac{\sqrt{T_x}}{\sqrt{T_t} - \sqrt{T_b}} \, n\pi \tag{25}$$

4.4 Positions of Nodes and Anti-Nodes

At the *nodes* the riser lateral displacement "y" is zero. Hence from Equation (16):

$$z_k - z_b = k\pi \tag{26}$$

where "k" takes integer values between zero and n, the mode number.

For *adjacent nodes* (noted by subscripts k and $k + 1$):

$$z_{k+1} - z_k = \pi \tag{27}$$

Hence from Equations (25) and (26):

$$\sqrt{T_{k+1}} - \sqrt{T_k} = \frac{\sqrt{T_t} - \sqrt{T_b}}{n} \tag{28}$$

At the *anti-nodes* the amplitudes are a maximum. Hence from Equation (16):

$$z_a - z_b = (2a - 1)\frac{\pi}{2} \tag{29}$$

where "a" takes integer values between 1 and n, the mode number.

From Equations (26) and (29), for the *anti-node "a"* between *adjacent nodes* "k" and "$k + 1$":

$$z_{k+1} - z_a = z_a - z_k = \frac{\pi}{2} \tag{30}$$

Hence from Equation (25):

$$\sqrt{T_{k+1}} - \sqrt{T_a} = \sqrt{T_a} - \sqrt{T_k} = \frac{\sqrt{T_t} - \sqrt{T_b}}{2n} \tag{31}$$

Hence for Mode "n", the scale of $\sqrt{\text{Tension}}$, between the riser top end $\left(\sqrt{T_t}\right)$ and the riser foot $\left(\sqrt{T_b}\right)$ is divided into "$2\,n$" equal intervals by all the nodes and anti-nodes. This allows the tensions and positions of all the nodes and anti-nodes to be found very easily.

4.5 Mean Celerities between Adjacent Nodes

The transmission time $t_{k,\,k+1}$ of transverse waves between any two adjacent nodes (subscripts k and $k + 1$) is equal to half the natural period of the mode *(see Section 1.1)*. Hence from Equation (19):

$$t_{k,k+1} = \frac{T_{p_n}}{2} = \frac{2\sqrt{m}}{w}\left[\frac{\sqrt{T_t} - \sqrt{T_b}}{n}\right] \tag{32}$$

Calling $L_{k,\,k+1}$ the distance between the two nodes, and noting that $wL_{k,\,k+1} = T_{k+1} - T_k$ then from Equation (28):

$$t_{k,k+1} = \frac{2\sqrt{m}}{w}\left[\sqrt{T_{k+1}} - \sqrt{T_k}\right] = \frac{2\sqrt{m}.L_{k,k+1}}{\left[\sqrt{T_{k+1}} + \sqrt{T_k}\right]} \tag{33}$$

but from Equation (31):

$$\sqrt{T_a} = \frac{\sqrt{T_{k+1}} + \sqrt{T_k}}{2} \tag{34}$$

where T_a is the tension at the intermediate anti-node.

Hence:

$$t_{k,k+1} = \frac{L_{k,k+1}}{\sqrt{T_a / m}} \tag{35}$$

Thus the mean celerity between adjacent nodes:

$$c_{m_{k,k+1}} = \frac{L_{k,k+1}}{t_{k,k+1}} = \sqrt{T_a / m} \tag{36}$$

This result can also be obtained by *assuming* that the celerity at all points of the riser is given by $c_x = \sqrt{T_x / m}$, and then integrating over the length between adjacent nodes in order to find the mean celerity. This proves that such an assumption is coherent with Equation (16) and thus with Equation (14).

As will be seen in Section 6, the celerity corresponding to the unmodified equation *(Eq. (9))* is slightly different from $\sqrt{T_x / m}$.

4.6 Bottom end Angle

The slope of the riser can be found by differentiating Equation (16) which gives:

$$\frac{dy}{dx} = Y_a \sqrt{\frac{m\omega_n^2}{T_x}} \cos(z_x - z_b) \qquad (37)$$

Thus at the nodes:

$$\left(\frac{dy}{dx}\right)_{\text{nodes}} = \pm Y_a \sqrt{\frac{m\omega_n^2}{T_x}} \qquad (38)$$

Hence the bottom end angle:

$$\theta_b = \pm Y_a \sqrt{\frac{m\omega_n^2}{T_b}} \qquad (39)$$

It is interesting to note that the riser bottom end angle as given by Equation (39) depends on four parameters, none of which is related to the water depth or riser length.

The above is particularly striking for drilling risers. Amplitude (Y_a) is approximately equal to the riser hydrodynamic diameter (*i.e.* diameter of buoyancy units). The bottom end tension of a drilling riser is normally chosen to be just sufficient to lift clear the LMRP in case of riser disconnect. Hence it is independent of water depth. Likewise the riser linear mass (including contents and added mass) does not increase necessarily with water depth. The natural circular frequency which may be excited depends on the riser hydraulic diameter and current velocity according to the Strouhal relation *(see Eq. (1))*.

Equation (39) can be further simplified. From Equation (32):

$$\omega_n = \frac{2\pi}{T_{p_n}} = \frac{\pi}{t_{k,k+1}} \qquad (40)$$

Calling $L_{b,b+1}$ the length between the riser foot and the first node above it, and T_{a_1} the tension at the intermediate anti-node, then from Equations (35) and (40):

$$\omega_n = \pi \frac{\sqrt{T_{a_1}/m}}{L_{b,b+1}} \qquad (41)$$

substitution in Equation (39) gives:

$$\theta_b = \pm Y_a \frac{\pi}{L_{b,b+1}} \sqrt{\frac{T_{a_1}}{T_b}} \qquad (42)$$

Finally the bottom end angle depends on geometrical parameters of the riser profile (riser amplitude and height of first node) amplified by $\sqrt{T_{a_1}/T_b}$. (Note: if curvature were

completely circular between the riser foot and the 1st node, the bottom end angle would be given by $4Y_a/L_{b,b+1}$. For a pure sinusoid it would be equal to $\pi Y_a/L_{b,b+1}$.

4.7 Riser Curvature (1/R) at the Anti-Nodes

Since riser curvature $1/R = d^2y/dx^2$, differentiation of Equation (37) yields:

$$\frac{1}{R} = Y_a \frac{m\omega_n^2}{T_x} \left\{ \sin(z_x - z_b) + \frac{\cos(z_x - z_b)}{z_x} \right\} \qquad (43)$$

At the anti-nodes {} = 1 and the curvature is then given by:

$$\frac{1}{R} = Y_a \frac{m\omega_n^2}{T_a} \qquad (44)$$

Since tension decreases with depth, Equation (44) has its greatest value at the lowest anti-node, where from Equation (41):

$$\frac{1}{R} = Y_a \left(\frac{\pi}{L_{b,b+1}}\right)^2 \qquad (45)$$

Thus the curvature at the lowest anti-node depends *only* on the amplitude of the riser vibration and the height of the first node. Neither water depth nor riser length enter into the equation.

(Note: if curvature were completely circular between the riser foot and the 1st node, it would be equal to $8Y_a/L_{b,b+1}^2$. For a pure sinusoid it would also be given by Equation (45)).

4.8 Maximum Riser Curvature (1/R)

Since riser tension decreases with depth the *maximum curvature* will occur for $d^3y/dx^3 = 0$ at some point *below* the lowest anti-node.

Differentiation of Equation (43) shows this occurs for $z_x = z_{c_{\max}}$ where

$$\tan(z_{c_{\max}} - z_b) = \frac{z_{c_{\max}}}{3} - \frac{1}{z_{c_{\max}}} \qquad (46)$$

$z_{c_{\max}}$ depends only on z_b and can be found by iteration. The corresponding tension can then be found *(from Eq. (25))*. Finally its relative position (between the riser foot and the first anti-node) and the relative value of maximum curvature (compared to curvature at the first anti-node) only depend on z_b.

For very high values of z_b maximum curvature is close to the lowest anti-node and there is negligible curvature amplification. As z_b decreases, the position of maximum

curvature gets closer and closer to the riser foot and curvature amplification increases.

- For $z_b = 7$, it is at the 3/4 position (above the riser foot) and the curvature amplification factor is equal to 1.07.
- For $z_b = 3.3$, it is at the mid-height; with curvature amplification equal to 1.25.
- For $z_b = 2.2$, it is at the quarter-point; with curvature amplification of 1.57.
- For $z_b = \sqrt{3}$, it is theoretically at the riser foot; with curvature amplification of 2.1.

For z_b to be equal to $\sqrt{3}$, it can be shown that the top tension factor T_t / wL must be less than 1.15 for 1st Mode vibrations; less than 1.05 for 2nd Mode vibrations and even less for higher modes. These cases are of little practical interest.

5 SIMPLIFIED ANALYSIS WITH FLEXURAL RIGIDITY *(EI)*

In Section 2 the solution for a *tensioned beam* under *constant tension* was presented. It is interesting to see if similar equations can be justified for such a beam under *uniformly varying* tension. Equation (2) with the "dy/dx" term modified *(as in Section 4)* becomes:

$$EI \cdot \frac{d^4 y}{dx^4} - T_x \frac{d^2 y}{dx^2} - \left(\frac{1}{2}\right) w \frac{dy}{dx} + m \frac{d^2 y}{dt^2} = 0 \qquad (47)$$

The procedure consists firstly of replacing T_x by $T'_x = T_x + Q$ in Equation (10) *between nodes*, where Q is a constant to be determined (values of Q being different for each pair of nodes); and secondly of *assuming* that there is a solution between nodes of the form:

$$y = Y_a \sin(z'_x - z'_k) \sin(\omega'_n t) \qquad (48)$$

Primed values of all parameters (T'_k, T'_a, z', ω'_n, c', etc.) apply to the case with rigidity *(EI)*. Since the *assumed form* of the solution is the same as in Section 4, the equations of that section can be applied *between pairs of nodes* (providing primed values are used throughout). Substitution of Equation (48) in Equation (47) leads to the requirement:

$$EI \frac{d^2 y}{dx^2} + Qy = 0 \qquad (49)$$

The first term of Equation (49) is the bending moment in the riser, which is thus replaced by a force Q acting at distance y from the riser axis *i.e.* along the axis of the *deflected* riser, which is what is already implied by the initial assumption above.

A "mean" *constant* value of Q is required. This can be found by integrating Equation (49) between adjacent nodes (k to $k + 1$). From Equation (48) this leads to:

$$EI \frac{2m\omega'^2_n}{w} \left[\frac{\cos(z'_x - z'_k)}{z'_x} \right]_k^{k+1}$$
$$= Q \frac{w}{2m\omega'^2_n} \left[z'_x \cos(z'_x - z'_k) - \sin(z'_x - z'_k) \right]_k^{k+1} \qquad (50)$$

hence from Equation (27):

$$EI \frac{2m\omega'^2_n}{w} \left[\frac{1}{z'_{k+1}} + \frac{1}{z'_k} \right] = Q \frac{w}{2m\omega'^2_n} \left[z'_{k+1} + z'_k \right] \qquad (51)$$

Since the transmission time between adjacent nodes is equal to half the modal period, it follows that:

$$\omega'_n = \frac{2}{T'_{p_n}} \pi = \left(\frac{c'_m}{L'_{k,k+1}} \right) \pi \qquad (52)$$

Equations (10), (51), (52) give:

$$Q = \left[\frac{2m\omega'^2_n}{w} \right]^2 \frac{EI}{z'_k \cdot z'_{k+1}} = m \left(\frac{\pi . c'_m}{L'_{k,k+1}} \right)^2 \frac{EI}{\sqrt{T'_k T'_{k+1}}} \qquad (53)$$

Finally from Equation (36):

$$Q = \left\{ \frac{T'_a}{\sqrt{T'_k T'_{k+1}}} \right\} \left(\frac{\pi}{L'_{k,k+1}} \right)^2 EI \qquad (54)$$

From Equation (34), factor { } in Equation (54) becomes:

$$\{ \ \} = \left\{ \frac{1}{4} \left[\sqrt[4]{\frac{T'_{k+1}}{T'_k}} + \sqrt[4]{\frac{T'_k}{T'_{k+1}}} \right]^2 \right\} \qquad (55)$$

This factor is equal to unity for the cases of constant tension and zero tension, which is coherent with the requirements of Section 2. In fact the factor can never differ greatly from 1 for practical riser cases. For the example in Appendix, it varies from 1.4 for Mode 1 (for which *EI* has negligible effect), to 1.03 for the length above the riser foot for Mode 5. It approaches more closely to 1 for higher modes.

The mean celerity between adjacent nodes is given by Equation 36 using primed values T'_a and c'_m. Between nodes k, $k + 1$:

$$c'_m = \sqrt{\frac{T'_a}{m}} = \frac{\sqrt{T_{k+1} + Q} + \sqrt{T_k + Q}}{2\sqrt{m}} \qquad (56)$$

Thus:

$$c'_m = \frac{\sqrt{(c_{k+1})^2_{cable} + c^2_{beam}} + \sqrt{(c_k)^2_{cable} + c^2_{beam}}}{2} \qquad (57)$$

where $c^2_{beam} = Q/m$. Tension is lowest between the riser foot and the first node. Hence that is where *cable celerities* have their *lowest* values. It is also where the inter-nodal distance is shortest, hence where Q is greatest *(see Eq. (54))* and hence where *beam celerity is greatest*. Therefore it is between the riser foot and the first node that *EI* has its greatest effect.

Since the value of Q is different for each pair of nodes, the procedures of Sections 4.1, 4.2 and 4.5 cannot be used to find the natural periods and the positions of nodes. Another approach must be used.

The modal period and the distance between nodes can be expressed in terms of the values (between nodes) of the mean celerities or of $\sqrt{T'_a}$ *(see Eq. (36))*. Since the transmission time between adjacent nodes is equal to half the modal period, and since the sum of the nodal lengths is equal to the riser length, it follows that:

$$L \; = \; \sum_1^n L'_i \; = \; \sum_1^n \left(\frac{T'_{p_n}}{2} c'_{m_i} \right) \tag{58}$$

hence the modal period is given by:

$$T'_{p_n} \; = \; \frac{2L}{\sum_1^n c'_{m_i}} = \frac{2L\sqrt{m}}{\sum_1^n \sqrt{T'_a}} \tag{59}$$

and the lengths between nodes:

$$L'_{k,k+1} \; = \; \frac{T'_{p_n}}{2} c'_{m_{k,k+1}} \; = \; \frac{L}{\sum_1^n c'_{m_i}} c'_{m_{k,k+1}} \tag{60}$$

Hence:

$$L'_{k,k+1} \; = \; \frac{L}{\sum_1^n \sqrt{T'_a}} \sqrt{T'_a} \tag{61}$$

Equation (59) gives the modified modal periods. The modified lengths between nodes can be calculated from either Equations (60) or (61). The bottom end angle and the riser curvature can then be found from the Equations (42) and (45) of Section 4 using the primed parameters.

6 VALIDATION

The above equations have been validated by comparing results for different cases using four methods of calculation:
- "simplified analysis" *(as presented in Section 4)*,
- "Bessel analysis" *(Section 3)*;
- finite element analysis with "Deeplines";
- "simplified analysis (with *EI*)" *(Section 5)*.

An example is given in Appendix for a large diameter drilling riser operating in deep water with very low top tension. Modal periods are presented in Table 1. Detailed results of node heights, bottom end angles and riser curvature for the 5th Mode are compared in Tables 2 to 6.

The principal results (height of lowest node, curvature at lowest anti-node and angle at riser foot) are compared in Table 7 for all methods except "Bessel" for various modes between 1 and 50.

Differences between results of the "simplified analysis" and the "Bessel analysis" are solely due to the halving of the second term of Equation (9).

TABLE 1

Riser natural periods for Modes between 1 and 50

Riser natural periods (s)								
	Mode 1	**Mode 2**	**Mode 3**	**Mode 4**	**Mode 5**	**Mode 6**	**Mode 8**	**Mode 10**
"Simplified analysis" (cable) Section 4	**77.5**	**38.7**	**25.8**	**19.4**	**15.5**	**12.9**	**9.7**	**7.7**
"Bessel analysis"	78.8	38.9	25.9	19.4	15.5	12.9	9.7	-
"Deeplines"	78.1	38.6	25.7	19.2	15.4	12.7	9.4	7.5
"Simplified analysis" (with *EI*) Section 5	**77.5**	**38.7**	**25.8**	**19.3**	**15.4**	**12.8**	**9.5**	**7.6**

	Mode 15	**Mode 20**	**Mode 25**	**Mode 30**	**Mode 35**	**Mode 40**	**Mode 45**	**Mode 50**
"Simplified analysis" (cable) Section 4	**5.2**	**3.87**	**3.10**	**2.58**	**2.21**	**1.94**	**1.72**	**1.55**
"Deeplines"	4.8	3.52	2.74	2.21	1.83	1.54	1.32	1.15
"Simplified analysis" (with *EI*) Section 5	**4.9**	**3.54**	**2.74**	**2.21**	**1.83**	**1.54**	**1.32**	**1.15**

TABLE 2

Riser vibration in 5th Mode.

Comparison of positions of nodes and anti-nodes

| | "Simplified analysis" Section 4 | | | | "Bessel analysis" | | "Deeplines" | |
| | (Tension)$^{1/2}$ (tf)1/2 | Tension (tf) | Height above riser foot (m) | | Height above riser foot (m) | | Height above riser foot (m) | |
			node	anti-node	node	anti-node	node	anti-node
Node 5	27.75	**770**	**2000**		2000		2000	
	25.81	**666.2**		**1703**		1699		1701
Node 4	23.87	**569.9**	**1428**		1428		1432	
	21.93	**481.1**		**1174**		1170		1175
Node 3	20.00	**399.8**	**942**		942		948	
	18.06	**326.1**		**731**		727		734
Node 2	16.12	**259.9**	**542**		542		549	
	14.18	**201.1**		**374**		370		377
Node 1	12.24	**149.9**	**228**		228		234	
	10.30	**106.2**		**103**		99		104
Node 0	8.37	**70**	**0**		0		0	

TABLE 3

Riser vibration in 5th mode.

Comparison of values of dimensionless parameter "z_x"

| | "Simplified analysis" | | | "Bessel analysis" | |
| | (Tension)$^{1/2}$ (tf)1/2 | z_x (Eq. 25) | | z_x | |
		Node	anti-node	node	anti-node
Node 5	27.75	**22.489**		22.470	
	25.81		**20.918**		20.876
Node 4	23.87	**19.347**		19.330	
	21.93		**17.776**		17.732
Node 3	20.00	**16.205**		16.189	
	18.06		**14.635**		14.585
Node 2	16.12	**13.064**		13.050	
	14.18		**11.493**		11.437
Node 1	12.24	**9.922**		9.911	
	10.30		**8.351**		8.283
Node 0	8.37	**6.781**		6.775	

Differences between results of "*Deeplines*" and of "simplified analysis (with *EI*)" are due to the approximations introduced in Section 5.

6.1 Riser Natural Periods

Riser natural periods obtained by the four methods are compared in Table 1 for various modes between 1 and 50. "Bessel analysis" could not be used beyond the eighth mode.

Agreement between natural periods calculated by the "simplified analysis" *(Eqs (22) and (23))* and the "Bessel analysis" improves as the mode number increases (1.7% difference for the fundamental; 0.5% for Mode 2; negligible for Mode 3 and above).

The modal periods calculated by "Deeplines" and the "simplified analysis with (*EI*)" are in remarkably good agreement. They are shorter than those given by the "Bessel analysis" (up to Mode 8) because of the slight increase in celerity caused by flexural rigidity. The influence of flexural rigidity becomes significant for Modes 15 and above. It increases with the mode number.

6.2 Positions of Nodes and Anti-Nodes

Table 2 gives the positions of the nodes and anti-nodes found by the first three methods. According to the "simplified analysis" their positions are defined by equal intervals of $\sqrt{Tension}$ between the riser head and foot. The positions for the *nodes* agree with those of the "Bessel analysis" to within a few centimetres.

Differences between results of the "Bessel analysis" and those obtained with "Deeplines" are due to the effect of riser flexural rigidity (*EI*). (Results obtained with "Deeplines" *without* flexural rigidity were found to be in good agreement with those of the "Bessel analysis" and are not presented separately in the Appendix).

TABLE 4

"Simplified analysis (with *EI)*".

Vibration in 5th Mode. Node heights and modal period *(see Section 5)*

Between nodes	T_a (tf) Table 2	L_n (m) Table 2	Q (tf) Eq. (54)	$\sqrt{T_a'}$ (tf)$^{1/2}$ Eq. (34)	T_a' (tf)	L_n' (m) Eq. (61)	Node	Height above riser foot (m)
4 to riser head	666.2	571.7	1.0	25.84	668.0	567.7	Riser head	2000
3 to 4	481.1	485.9	1.38	22.01	484.4	483.4	Node 4	1432.3
2 to 3	326.1	400.0	2.03	18.18	330.6	399.3	Node 3	948.9
1 to 2	201.1	314.13	3.27	14.38	206.7	315.8	Node 2	549.6
Riser foot to 1	106.2	228.3	6.06	10.64	113.3	233.8	Node 1	233.8
				$\Sigma = 91.05$		$\Sigma = 2000$	Riser foot	0

Modal period with rigidity *(Eq.(59))*: Tp = 2 x 2000 $\sqrt{1.2}$ / (91.05 $\sqrt{g}$) = 15.4 *s*

TABLE 5

Riser vibration in 5th Mode.

Angles at riser foot

Angles at riser foot			
"Simplified analysis" (cable) Section 4	"Bessel analysis"	"Deeplines"	"Simplifed analysis (with *EI)*" Section 5
0.97°	1.07°	0.93°	**0.94°**

TABLE 6

Riser vibration in 5th Mode.

Curvature (1/*R*) at points below lowest anti-node

Height above riser foot *(m)*	"simplified analysis" (cable) Section 4 *m*$^{-1}$	"Bessel analysis" *m*$^{-1}$	"Deeplines" *m*$^{-1}$	"Simplified analysis" (with *EI)* Section 5 *m*$^{-1}$
Anti-node	0.00019	0.00019	0.00018	0.00018
90	0.00020	0.00020	0.00019	0.00019
77	0.00020	0.00021	0.00020	0.00019
63	0.00020	0.00022	0.00020	0.00019
50	0.00019	0.00021	0.00018	0.00017
40	0.00017	0.00020	0.00017	0.00016
30	0.00015	0.00019	0.00014	0.00014

TABLE 7

For Modes between 1 and 50:
height of 1st node; curvature at lowest anti-node; angle at riser foot

Mode	Height of 1st node (m)			Curvature (m^{-1}) at the lowest anti-node			Angle at riser foot		
	Simplified analysis (cable)	Simplified analysis (with *EI*)	*Deeplines* (with *EI*)	Simplified analysis (cable)	Simplified analysis (with *EI*)	*Deeplines* (with *EI*)	Simplified analysis (cable)	Simplified analysis (with *EI*)	*Deeplines* (with *EI*)
1	2000	**2000**	2000	0.0000025	0.0000025	0.0000027	0.19°	0.19°	0.26°
2	731.7	**732.6**	731.4	0.000018	0.000018	0.000019	0.39°	0.39°	0.44°
3	428.1	**430.4**	430.7	0.000054	0.000053	0.000055	0.58°	0.58°	0.61°
4	298.7	**302.5**	303.3	0.00011	0.00011	0.00011	0.78°	0.76°	0.77°
5	228.3	**233.8**	234.5	0.00019	0.00018	0.00018	0.97°	0.94°	0.93°
10	103.4	**114.6**	115.1	0.00092	0.00075	0.00075	1.94°	1.72°	1.67°
20	49.0	**64.0**	64.0	0.0041	0.0024	0.0023	3.88°	2.92°	2.87°
30	32.1	**47.1**	47.2	0.0096	0.0044	0.0042	5.83°	3.91°	3.84°
40	23.8	**38.1**	38.1	0.0174	0.0068	0.0064	7.77°	4.78°	4.73°
50	19.4	**32.2**	32.1	0.0263	0.0095	0.0088	9.52°	5.64°	5.60°

For the *anti-nodes* agreement is less good (4 to 5 m difference for each anti-node). This is because the middle term of Equation (9) *does* contribute to the celerity of the transverse waves. Between any node and the anti-node below it, this term combines with the restoring force *(see Fig. 3)* and has the effect of slightly increasing celerity. Between the anti-node and the node below it, the opposite is the case. Since this term has been halved for the "simplified analysis" the effect is reduced (compared with the "Bessel analysis") and as a result the anti-nodes are raised slightly.

Between two adjacent *nodes* the two effects virtually balance each other, hence the excellent agreement for the positions of the nodes.

The *nodes* given by "Deeplines" are higher than those found by the "Bessel analysis". Flexural rigidity has the effect of increasing the celerity, and this effect is greatest at the riser lower end where tension is lowest. This has the effect of slightly raising all the nodes.

The values of the dimensionless parameter "*z*" for the "simplified analysis" *(given by Eq. (24))* and for the "Bessel analysis" are given in Table 3 for comparison.

Table 4 presents the calculation of the modified node heights (and natural period), according to the "simplified analysis (with *EI*)" *(Section 5)*. This requires a number of iterations which increases with the mode number. For the 5th Mode results presented in Table 4, three iterations were required. Calculated node heights agree with the results of "Deeplines" given in Table 2 to within 1 m.

6.3 Angles at the Riser Foot

Table 5 gives the riser bottom end angles for the 5th Mode as calculated by the four methods.

"Deeplines" and the "simplified analysis (with *EI*)" gives the smallest values which is not surprising since it is at the riser bottom end that flexural rigidity has it greatest effect [9].

The "middle term" is greater in Equation (9) than in Equation (14). This leads to a greater calculated angle for the "Bessel analysis" than for the "simplified analysis".

6.4 Curvature at the Lowest Anti-Node and Below

Table 6 gives the riser curvature (1/*R*) calculated by the four methods. There is good agreement between them. Flexural rigidity reduces curvature slightly for "Deeplines" and "simplified analysis (with *EI*)" as would be expected.

The position of *maximum curvature* is about 40 m below the lowest anti-node according to the "Bessel analysis". For the others it is about 25 m below it.

6.5 Influence of Rigidity (*EI*)

Equations (41) and (45) show that the principal parameter that influences maximum curvature and bottom end angle is the height of the lowest node.

As shown in Section 5, *EI* increases celerity between nodes *(Eqs (54), (56) and (57))*. This effect is greatest at the

riser lower end and reduces progressively with height above the riser foot. As can be deduced from Equation (60), this causes inter-nodal lengths to be increased in the lower part of the riser and decreased in the upper part (*see Table 4*). Hence all nodes are raised.

For modes between 1 and 50, Table 7 compares values of the following, as calculated by the different methods: height of the lowest node, curvature at lowest anti-node and angle at the riser foot.

Tabulated values show excellent agreement between "Deeplines" and the "simplified analysis with (*EI*)" for all modes.

At low modes all three methods agree which is not surprising since *EI* then has negligible effect. The influence of the rigidity *EI* can be seen to increase progressively with the mode number.

SUMMARY AND CONCLUSIONS

This paper has attempted to understand the physics of riser modal vibration of the type induced by VIV using an analytical approach based principally on two simplifications. The first consists of neglecting flexural rigidity and treating the riser as a tensioned cable. The second consists of slightly modifying a term of little significance in the basic vibration equation.

The method has led to very simple formulae for all the phenomena of interest, for a riser with *uniform* character-istics. Extension of the method to include the effect of flexural rigidity (*EI*) in a riser with varying tension has also been presented in Section 5.

The results obtained have been found to be in good agreement with more precise but more complicated analytical calculations involving Bessel functions, and with results of the "Deeplines" finite element riser analysis program.

Given the above simplifications the principal conclusions are as follows:

– the mean celerity in the riser is equal to the mean of the celerities at the riser extremities *(Eq. (21))*;

– the riser fundamental (1st Mode) natural period is the time required for a transverse wave to run twice the length of the riser. Hence it is equal to twice the riser length divided by the mean celerity *(Eq. (22))*;

– natural periods of higher modes are equal to the 1st Mode natural period divided by the mode number *(Eq. (23))*;

– the nodes and the anti-nodes divide the scale of $\sqrt{Tension}$ between the riser extremities into equal intervals. For the "nth" Mode there are "2 *n*" such intervals *(Eq. (31))*;

– the maximum angle at the riser foot is independent of the water depth. It depends on geometrical factors namely: the amplitude of the vibration; the height of the first node above the riser foot; and on the tension ratio between the first anti-node and the riser foot *(Eq. (42))*;

– curvature at the lowest anti-node is independent of water depth. It only depends on the amplitude of the vibration and the height of the first node *(Eq. (45))*;

– maximum curvature occurs between the riser foot and the lowest anti-node. Its precise position and value can be found by iteration *(Eq. (46))*.

In Section 5 it is shown that flexural rigidity *EI* can be treated as an equivalent additional axial tension between nodes. This causes celerities to be increased, particularly in the lower part of the riser. As a result node heights are raised which has the effect of reducing maximum curvature and angles at the riser foot. Natural periods are reduced.

The paper shows that deep water modal vibrations are little different from such vibrations in lesser depths. Water depth is not the major factor in determining the principal consequences of such vibrations. Far more significant is the height of the first node.

What does increase with water depth is the probability that a modal period will be close to a potential excitation period, given by the Strouhal relation *(Eq. (1))*. But then the probability of damping (due to nonuniform current profile and direction) also increases with water depth. These two important aspects of riser VIV response are beyond the scope of this paper.

The above conclusions are valid for deepwater vertical risers with *uniform* characteristics. They help contribute to the understanding of the more general case of a riser with *non-uniform* characteristics, which can only be treated by more sophisticated methods such as finite element analysis.

REFERENCES

1 Allen, D.W. (1998) Vortex-Induced Vibration of Deepwater Risers, Paper OTC 8703. *Offshore Technology Conference*, Houston.

2 Furnes, G.K., Hassanein, T., Halse, K.H. and Eriksen, M. (1998) A Field Study of Flow Induced Vibrations on a Deepwater Drilling Riser. Paper OTC 8702, *Offshore Technology Conference*, Houston

3 Kaasen, K.E., Lie, H., Solaas, F. and Vandiver, J.K. (2000) Norwegian Deepwater Program: Analysis of Vortex Induced Vibrations of Marine Risers Based on Full-Scale Measurements. Paper OTC 11997, *Offshore Technology Conference*, Houston.

4 Halse, K.H. (2000) Norwegian Deepwater Program: Improved Predictions of Vortex Induced Vibrations. Paper OTC 11996, *Offshore Technology Conference*, Houston

5 Cornut, S.F.A. and Vandiver, J.K. (2000) Offshore VIV Monitoring at Schiehallion – Analysis of Riser VIV Response. Paper OMAE 2000/Pipe-5022, *Offshore Mechanics and Arctic Engineering Conference*, New Orleans.

6 Brooks, I.H. (1987) A Pragmatic Approach to Vortex-Induced Vibrations of a Drilling Riser. Paper OTC 5522, *Offshore Technology Conference*, Houston.

7 Lie, H., Mo, K. and Vandiver, J.K. (1998) VIV Model Test of a Bare- and a Staggered Buoyancy Riser in a Rotating Rig. Paper OTC 8700, *Offshore Technology Conference*, Houston.

8 Huse, E., Kleiven, G. and Nielsen, F. (1998) Large Scale Model Testing of Deep Sea Risers. Paper OTC 8701, *Off-Shore Technology Conference*, Houston.

9 Sparks, C.P. (1980) Mechanical Behavior of Marine Risers. Mode of Influence of Principal Parameters. *Transactions of ASME, Journal of Energy Resources Technology*, **102**, 214-222.

10 Biolley, F., Heutier, J.M., Berhault, C., Le Buhan, P. and Morin, G. (1998) Fully Coupled Dynamic Analysis of Rigid Lines and Floaters Behaviour in Deep Water. *Proceedings of the Eighth International Offshore and Polar Engineering Conference.*

11 Blevins, R.D. (1977) *Flow Induced Vibrations*, Van Norstrand, New York.

12 Sarpkaya,T. and Isaacson, M. (1981) *Mechanics of Wave Forces on Offshore Structures*, Van Norstrand, New York.

13 Strouhal, V. (1878) Über eine besondere Art der Tonerregung. *Ann. Phys. Und Chemie*, New Series.

14 Timoshenko, S., (1955) *Vibration Problems in Engineering*, Nostrand.

Final manuscript received in July 2001

APPENDIX

Modal Vibration of a Deepwater Drilling Riser. Comparison between Analyses

Results obtained by the "simplified analysis", "Bessel analysis", the "Deeplines" riser program and "simplified analysis with (with *EI*)" are compared for a drilling riser with the characteristics given below.

Example Riser Characteristics

Riser length	(*L*)	2000 m
Riser pipe diameter		0.5588 m (22")
wall thickness		0.0254 m (1")
flexural rigidity	(*EI*)	318.6×10^6 N-m^2 (32 477 tonnes f-m^2)
hydraulic diameter		1 m
Apparent linear weight	(*w*)	3,433.5 N/m (0.35 tonnes f/m)
Total apparent weight	(*wL*)	6.867×10^6 N

Top tension factor	(*T_t*/*wL*)	1.1
Top end effective tension	(*T_t*)	7.5537×10^6 N (770 tonnes f)
Bottom end effective tension	(*T_b*)	0.6867×10^6 N (70 tf)
Mass (+ added mass)	(*m*)	1200 kg/m (1.2 tonnes/m).

General Parameters

Amplitude of vibrations	(*Y_a*)	1 m
Gravitational acceleration	(*g*)	9.81 m/s.